Long-range electroweak amplitudes of single hadrons from Euclidean finite-volume correlation functions

Alessandro Baroni,[1,2,*] Raúl A. Briceño,[3,4,†] Zohreh Davoudi,[5,6,‡]
Maxwell T. Hansen,[7,§] and Matthias R. Schindler[2,¶]

[1] *Theoretical Division, Los Alamos National Laboratory, Los Alamos, New Mexico 87545, USA*
[2] *Department of Physics and Astronomy University of South Carolina, Columbia, South Carolina 29208, USA*
[3] *Thomas Jefferson National Accelerator Facility, Newport News, Virginia 23606, USA*
[4] *Department of Physics, Old Dominion University, Norfolk, Virginia 23529, USA*
[5] *Maryland Center for Fundamental Physics and Department of Physics, University of Maryland, College Park, Maryland 20742, USA*
[6] *RIKEN Center for Accelerator-based Sciences, Wako 351-0198, Japan*
[7] *Theoretical Physics Department, CERN, 1211 Geneva 23, Switzerland*

(Dated: September 19, 2019)

This work presents an all-orders relation between long-range matrix elements of single hadrons obtained from finite Euclidean spacetime correlation functions and infinite-volume Minkowski amplitudes, in the kinematic region where at most two single hadrons can simultaneously go on-shell. This relation can be understood as a two-step procedure. First, by removing contributions from on-shell one- and two-particle intermediate states, we establish a one-to-one mapping between finite-Euclidean spacetime four-point functions and their Minkowski counterparts. Second, we derive an exact relation between the finite-volume Minkowski four-point function to the infinite-volume Minkowski amplitude involving two current insertions. The necessary pieces to carry out these two steps can be obtained from dedicated calculations of relevant two- and three-point correlation functions. The formalism can be applied to matrix elements of stable particles with arbitrary quantum numbers, for all possible kinematics/virtualities below the first unaccounted threshold, as well as when single or multiple coupled channels are kinematically accessible in intermediate states, hence extending the formalism of Christ et al. in Phys.Rev. D91 114510 (2015). In addition to neutral mesons mixing and rare decays of pseudo-scalar mesons that were considered previously, the formalism presented can be applied to a wide class of lattice QCD studies, including Compton scattering, radiative corrections to the β decay of the nucleon and double-β decays of single hadrons.

PACS numbers: 12.38.-t 11.15.Ha, 12.38.Gc, 12.38.-t, 13.15.+g, 23.40.Bw, 13.60.Fz 12.15.-y

I. INTRODUCTION

Long-range electroweak matrix elements of hadrons play a central role in modern hadronic physics, from precision tests of the Standard Model (SM) to investigations into the inner structure of hadrons. Key examples of physical processes where theoretical constraints on such matrix elements are needed include Compton scattering, double-β decays, $K-\overline{K}$ oscillations and rare meson decays. Through deeply virtual Compton scattering, i.e., when a virtual photon scatters off a charged hadronic target and turns into a real photon, $\gamma^* h \to \gamma h$, one may extract the generalized parton distributions of the target hadron, as proposed by Ji [1]. Such a process can be studied at leading order in quantum electrodynamics (QED) by performing appropriate Fourier transforms of matrix elements involving time-displaced electromagnetic (EM) currents. Neutrinoless double

* abaro008@odu.edu
† rbriceno@jlab.org
‡ davoudi@umd.edu
§ maxwell.hansen@cern.ch
¶ mschindl@mailbox.sc.edu

beta decay is a hypothesized process through which two neutrons inside specific nuclear isotopes are transformed into protons without emitting neutrinos. This would only be possible if neutrinos are their own antiparticles, in other words they would have to be Majorana fermions, unlike any other fermion in the SM. There is a strong ongoing effort to find experimental evidence of such a lepton-violating process; for reviews see, e.g., Refs. [2–5]. There is a demand to place reliable theoretical constraints on the nuclear matrix elements relevant for this process, as well as a sister process in the SM in which two neutrinos are emitted in the final state. According to nuclear effective field theories [6–10], the $\pi^+ \to \pi^-$ inversion may be an important contributions to the $nn \to pp$ inversion process. As a result, lattice QCD studies of these processes have already started [11–13] and a class of these computations require computation of bi-local matrix elements [12–15]. These examples are just two of a broad class of observables which would require the evaluation of matrix elements of two displaced currents. Other examples include the computation the mass splitting among neutral mesons with displaced weak currents [16–19], rare decays of mesons such as $K \to \pi l^+ l^-$ [20] and $K \to \pi\nu\bar{\nu}$ [21, 22] with displaced weak and EM currents and displaced weak currents, respectively.[1]

Presently, the only reliable tool to study such matrix elements from the underlying theory is lattice QCD. Lattice QCD is a numerical method for statistically evaluating QCD correlation functions using Monte Carlo techniques in Euclidean spacetime.[2] This feature leads to two major challenges in accessing Minkowski amplitudes. The first challenge presents itself when aiming to evaluate matrix elements of currents that are displaced in time. In general, non-local Euclidean matrix elements are not equal to their Minkowski counterparts. As a result the relation between these quantities must be formally obtained. The second challenge is related to the fact that the eigenstates of the Hamiltonian in a finite spatial volume are discrete, even above multi-particle thresholds, while in the infinite volume there exists a continuum of states. These features alter the analytic structure of correlation functions dramatically. [3]

The two challenges described above are in fact correlated. Since the time-evolution operator depends on the time signature of spacetime and on the Hamiltonian itself, these two issues must, in general, be treated simultaneously. To understand this point, one can look at the example of a long-range matrix element involving a current placed at the origin, $J(0)$, and a second current applied at some later Euclidean time τ, $J_E(\tau)$. Inserting a complete set of finite-volume states characterized by momentum P_n and using the relation $J_E(\tau) = e^{H\tau} J(0) e^{-H\tau}$ where H is the Hamiltonian operator, the matrix element can be written as

$$\langle P_f; L|\, J_E(\tau) J(0) |P_i; L\rangle = \sum_n e^{-\tau(E_n - E_f)} \langle P_f; L|\, J(0) |P_n; L\rangle \langle P_n; L| J(0) |P_i; L\rangle, \tag{1}$$

where an initial and a final state with total momenta P_i and P_f, respectively, are considered in a finite spatial volume. In general, the Laplace transform of this matrix element will not coincide with the Minkowski infinite-volume counterpart. The latter is in general complex due to the branch cuts of multi-particle scattering states. On the other hand, the Laplace transform of Eq. (1) is purely real and has no branch cuts. Instead, it is simply a sum over contributions from poles.

To compare to the desired Minkowski amplitude, one must integrate Eq. 1 over all values of τ with a weighting factor of $e^{\tau\omega}$, where ω is the energy carried by the current. It turns out that in the kinematic region below multi-particle thresholds, the resultant single-hadron long-range amplitude in a finite Euclidean spacetime is exponentially close to its infinite Minkowski

[1] Further examples can be found, e.g., in a series of recent USQCD whitepapers [23–26].

[2] For exploratory studies of real-time dynamics in simple theories with classical computations based on Monte Carlo methods, and with quantum computations based on direct implementation of the Hamiltonian time evolution, see Refs. [27–30]. The generalization of these methods to QCD remains formally and practically challenging.

[3] Note, this is quite different to the case where the bi-local currents are displaced in space, where the analytic continuation is trivial [31] and finite-volume effects are exponentially suppressed [32].

spacetime counterpart [33, 34] with corrections that scale as $\mathcal{O}(e^{-m_\pi L})$, where m_π is the mass of the lightest hadron in the theory, the pion. This observation has made numerous calculations possible [33, 35–39], including the lattice QCD determinations of the hadron vacuum polarization (HVP) contribution to the anomalous magnetic moment of the muon. The first attempt to move beyond this kinematic restriction was made in the context of determining the long-range contributions to the $K_L - K_S$ mass splitting (those arising from physics at the scale of the charm quark mass and below), as presented in Refs. [16–18]. This framework has enabled preliminary determinations of the mass splitting of neutral Kaons via lattice QCD [19, 40–42]. Long-range matrix elements occurring in rare decays of the kaon, such as in $K \to \pi l^+ l^-$ and $K \to \pi\nu\bar{\nu}$ processes [20–22], and hadronic double-β decays [12–15], have also been studied in recent years.

The formalism presented in this paper goes beyond previous work by providing a general and non-perturbative mapping between quantities that are accessed via lattice QCD and the infinite-volume Minkowski long-range amplitudes. Inspired by the essential conclusion of Ref. [33], in which the hadron-vacuum polarization was shown to be accessible from Euclidean correlation functions below the hadronic production threshold, the central idea behind the present work is to build a relationship between the Minkowski and Euclidean four-point correlation functions via a straightforward analytic continuation, but to go beyond the kinematic constraint of Ref. [33]. This is done at the level of finite-volume correlation functions and is only possible if the contribution from on-shell intermediate states are first subtracted out. These contributions are indeed the origin of the fundamental difference in the analytic structure of the correlation functions.

We then provide a close form for the remaining additive piece needed to remove the power-law finite-volume effects and assured that the resultant amplitude has the right analytic structure. This correction is known exactly provided that the relevant finite-volume spectrum and $1 \to 1$ and $1 \to 2$ matrix elements are known. This can be achieved through preceding dedicated lattice QCD studies in the proper kinematic region. This step builds off two important formal developments: the Lüscher-like formalisms [43–51], which have permitted the determination of infinite-volume scattering amplitudes of two hadrons from lattice QCD spectra [52–64], as well as the non-perturbative relations between finite-volume matrix elements and electroweak amplitudes [49, 65–71].[4] Once these steps are all taken, one reaches the desired long-range Minkowski infinite-volume amplitude.

The approach developed in Refs. [16–18] in the context of determining the long-range contributions to the $K_L - K_S$ mass splitting and the CP-violating parameter ϵ_K is closely related. These studies identify artifacts associated with intermediate $\pi\pi$ states that may go on-shell via $K^0 \to \pi\pi \to \overline{K}^0$, leading to power-law finite-volume effects. Such artifacts can be removed once the physical on-shell $K^0 \to \pi\pi$ weak amplitude, as well as the physical elastic scattering amplitude for $\pi\pi \to \pi\pi$, are determined using other studies. Our work generalizes this formalism to arbitrary currents, generic incoming and outgoing single-hadron states and kinematics.

The results of this paper hold for arbitrary spins and quantum numbers of the single hadron undergoing the transition, and can be used to study kinematics above any number of two-particle thresholds. It therefore accounts for physical mixing among two-particle intermediate states due to strong interactions, moving the cutoff on the validity of the formalism to the first threshold involving production of three-particle states [76–82].[5] It also accounts for unphysical mixing among angular momentum states due to the reduced symmetry of a cubic volume. Last but not least, the formalism can be used to reduce systematic uncertainties of long-range matrix elements of hadrons even below two-particle thresholds, by identifying and removing contributions from intermediate states. A similar approach has been applied to the HVP computations via lattice QCD, where the knowledge of the $\pi\pi \to \pi\pi$ and $\gamma^* \to \pi\pi$ amplitudes allows to reduce the finite-volume effects, as suggested in Refs. [38, 39].

---

[4] For recent reviews on these formal developments and their numerical implementations, we point the readers to Refs. [72–75].

[5] Four-particle states if the transition of the single hadron to three-particle states is dynamically forbidden.

This paper is organized as follows. Sec. II introduces the main idea of this work accompanied by the framework that enables the matching between the finite-volume Euclidean four-point function and the a generic Minkowski infinite-volume bi-local matrix element. The ingredients of the framework presented will be explained in the following Sec. III, along with a recap of the two-hadron finite-volume formalism for scattering and transition amplitudes, leading to the identification of new power-law finite-volume effects in the hadronic four-point functions under study. In Sec. III A we provide a strong check on the formalism showing that the main result satisfies unitarity exactly. In order to demonstrate an application of the formalism, in Sec. IV we limit our attention to a single channel and evaluate numerically all the building blocks for a specific example. Sec. V summarizes the approach of this paper and offers a diagrammatic presentation of the workflow for achieving the long-range matrix element of interest from a corresponding lattice QCD computation.

II. THE RELATION BETWEEN FINITE-VOLUME EUCLIDEAN AND INFINITE-VOLUME MINKOWSKI AMPLITUDES

We begin by presenting the main result of this work, which can be compactly written as

$$\mathcal{T}(\omega, \boldsymbol{q}) = \int_{-\infty}^{\infty} d\tau\, e^{-\omega\tau}\, G^{\geq N}(\tau, \boldsymbol{q}, L) + \left[T^{<N}(\omega, \boldsymbol{q}, L) + \Delta T(\omega, \boldsymbol{q}, L)\right]_{\mathcal{M},\mathcal{H}} . \tag{2}$$

Here, the dependence of the functions on four-momenta of the initial and final hadron is left implicit. The left-hand side is the desired infinite-volume Minkowski amplitude, and the right-hand side is a carefully constructed combination of finite-volume Euclidean quantities: $G^{\geq N}(\tau, \boldsymbol{q}, L)$ is a four-point function evaluated for a range of Euclidean time, τ, while the last two terms contain information on the finite-volume spectrum and matrix elements of local operators, which can be obtained from finite-volume two- and three-point correlators. This section provides the exact definition of these functions and the relations among them.

Before defining the building blocks of Eq. (2), we introduce the basic notation that is used throughout. The 3-momentum of the incoming hadron state is denoted by $\boldsymbol{P}_i$ and that of the outgoing state is denoted by $\boldsymbol{P}_f$. The corresponding 4-momentum of the initial state is then given by

$$P_i^\mu \equiv (E_i, \boldsymbol{P}_i) = \left(\sqrt{M_i^2 + \boldsymbol{P}_i^2}, \boldsymbol{P}_i\right), \tag{3}$$

with an analogous relation for the final state with $i \to f$. Here, M_i and M_f are the physical masses. The hadronic states are denoted by $|P_i\rangle$ and $\langle P_f|$ and satisfy the standard relativistic normalization:

$$\langle P|P'\rangle = 2E\, (2\pi)^3\, \delta(\boldsymbol{P} - \boldsymbol{P}') . \tag{4}$$

Now consider two local, Minkowski-signature currents $\mathcal{J}_A(x)$ and $\mathcal{O}_B(x)$, with $x^\mu \equiv (t, \boldsymbol{x})$. Here, A and B are collective indices that specify the quantum numbers of the currents, e.g., they can specify scalar, axial, vector, tensor or other types of currents. The Lorentz structure of the currents plays no role in the following discussion. The goal is to obtain from an Euclidean finite-volume correlation function the infinite-volume amplitude appearing on the left hand side of Eq. (2),

$$\mathcal{T}(\omega, \boldsymbol{q}) \equiv i \int d^4x\, e^{-i\omega t + i\boldsymbol{q}\cdot\boldsymbol{x}}\, \langle P_f|\, \mathrm{T}\{\mathcal{J}_A(x)\mathcal{O}_B(0)\}\, |P_i\rangle_{\text{conn.}} , \tag{5}$$

where again the P_i and P_f dependence of the amplitude is made implicit. T in this relation denotes time ordering and the subscript conn. denotes that only the connected contributions to the matrix element are considered. This distinction will only be relevant in the forward limit

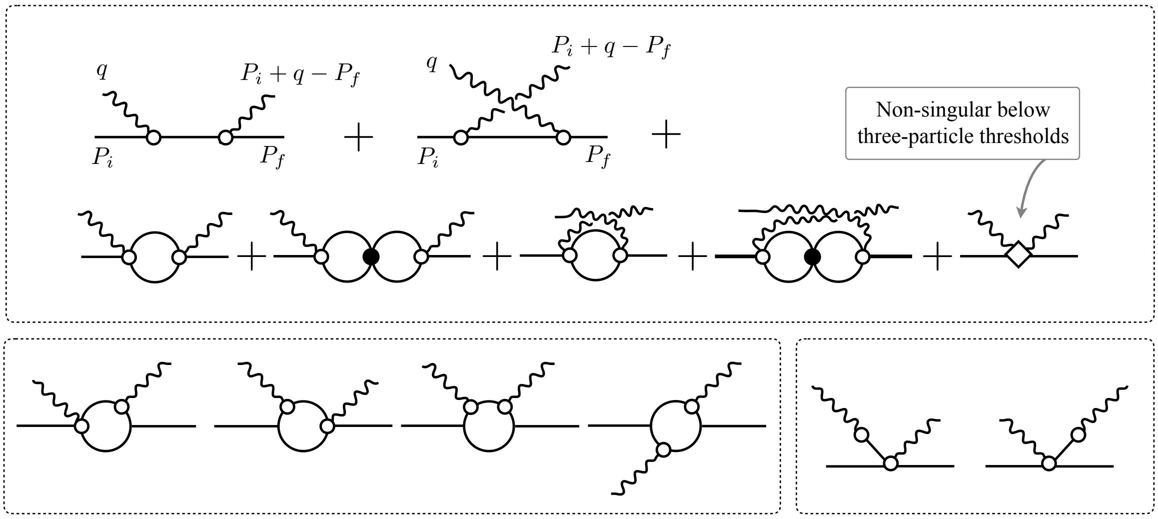

FIG. 1: A diagrammatic expansion of the Compton amplitude defined in Eq. (5) upon making contributions from single- and two-hadron intermediate states in the s- and u-channel diagram explicit. Contributions from z-channel diagrams, as well as other intermediate states in the s and u channels, are embedded in a two-hadron two-current vertex (the last diagram shown). This vertex is presents no two-particle singularities below three-particle production thresholds and is equivalent to its infinite-volume counterpart up to exponentially suppressed contributions in the spatial extent of the volume.

when $P_i = P_f$. In what follows we will make use of the all-orders diagrammatic representation of this amplitude, given in terms of various kernels in Fig. 1.

In a finite cubic volume with spatial extent L, and with periodic boundary conditions applied to all fields along the three spatial directions, the finite-volume shifts to the masses, M_i and M_f, are exponentially suppressed in L. Assuming $ML \gg 1$ for lightest particle in the theory, such corrections can be neglected. Therefore, in such a limit, the 4-vectors P_i and P_f also label the finite-volume states, denoted by $|P_i, L\rangle$ for the incoming hadron and $\langle P_f, L|$ for the outgoing hadron. We adopt the convention that finite-volume states are normalized to unity,

$$\langle P; L | P'; L\rangle = \delta_{\boldsymbol{P},\boldsymbol{P}'} \,, \tag{6}$$

where $\boldsymbol{P} = 2\pi \boldsymbol{n}/L$ and $\boldsymbol{P}' = 2\pi \boldsymbol{n}'/L$, with $\boldsymbol{n}, \boldsymbol{n}' \in \mathbb{Z}^3$. This means that the only difference between the infinite- and finite-volume single-hadron states with the same energy and momentum is a trivial normalization factor, cf. Eq. (4). Introducing $\mathcal{J}_A^E(\tau, \boldsymbol{x})$ and $\mathcal{O}_B^E(\tau, \boldsymbol{x})$ as Euclidean counterparts of the local currents in Eq. (5), one can write down a lattice QCD correlator most closely related to $\mathcal{T}$,

$$G_L(\tau, \boldsymbol{q}) \equiv i\, 2L^3 \sqrt{E_i E_f} \int_L d^3\boldsymbol{x}\, e^{-i\boldsymbol{q}\cdot\boldsymbol{x}} \, \langle P_f, L|\, \mathrm{T}_E\{\mathcal{J}_A^E(\tau, \boldsymbol{x}) \mathcal{O}_B^E(0)\}\, |P_i, L\rangle, \tag{7}$$

where in the forward limit, the disconnected contribution

$$G_L^{\mathrm{disc}}(\tau, \boldsymbol{q}) \equiv i\, 2L^3 \sqrt{E_i E_f} \langle P_f, L | P_i, L\rangle \int_L d^3\boldsymbol{x}\, e^{-i\boldsymbol{q}\cdot\boldsymbol{x}} \, \langle 0|\mathrm{T}_E\{\mathcal{J}_A^E(\tau, \boldsymbol{x}) \mathcal{O}_B^E(0)\}|0\rangle \tag{8}$$

must be subtracted from Eq. (7) in order to map to Eq. (5). The L subscript on the integrals implies that the integration is performed over a cubic volume with extent L. For notational brevity, the hadron momentum labels P_i and P_f are left out from the arguments of the correlators. Since at $\tau = 0$ the currents carry no information about the time, one can further assume a phase convention such that the Euclidean and Minkowski currents are identical at $\tau = 0$, i.e., $\mathcal{J}_A^E(0, \boldsymbol{x}) = \mathcal{J}_A(0, \boldsymbol{x})$ and $\mathcal{O}_B^E(0, \boldsymbol{x}) = \mathcal{O}_B(0, \boldsymbol{x})$.

To understand the issues in extracting $\mathcal{T}$ from G, it is instructive to first perform a spectral decomposition on the latter. Defining

$$c_n \equiv i\, 2L^3 \sqrt{E_i E_f} \int_L d^3\boldsymbol{x}\, e^{-i\boldsymbol{q}\cdot\boldsymbol{x}}\, \langle P_f, L|\mathcal{J}_A(0,\boldsymbol{x})|n, L\rangle\langle n, L|\mathcal{O}_B(0)|P_i, L\rangle\,, \tag{9}$$

$$\bar{c}_{\bar{n}} \equiv i\, 2L^3 \sqrt{E_i E_f} \int_L d^3\boldsymbol{x}\, e^{-i\boldsymbol{q}\cdot\boldsymbol{x}}\, \langle P_f, L|\mathcal{O}_B(0)|\bar{n}, L\rangle\langle \bar{n}, L|\mathcal{J}_A(0,\boldsymbol{x})|P_i, L\rangle\,, \tag{10}$$

one obtains

$$G_L(\tau,\boldsymbol{q}) \equiv \sum_{n=0}^{\infty} c_n\, \Theta(\tau)\, e^{-[E_n(L,\boldsymbol{P}_f-\boldsymbol{q})-E_f]|\tau|} + \sum_{\bar{n}=0}^{\infty} \bar{c}_{\bar{n}}\, \Theta(-\tau)\, e^{-[E_{\bar{n}}(L,\boldsymbol{P}_i+\boldsymbol{q})-E_i]|\tau|}\,. \tag{11}$$

The finite-volume states $|n, L\rangle$ and $|\bar{n}, L\rangle$ in Eqs. (9) and (10), and therefore the c_n and $\bar{c}_{\bar{n}}$ coefficients in Eq. (11), in general differ not only due to differing 3-momenta but also because of differing internal quantum numbers of the currents. For example, processes like $K \to \pi\gamma$ can be described if $\mathcal{J}_A = \mathcal{H}$ is a weak Hamiltonian and $\mathcal{O}_B = j_\mu$ is an electromagnetic current. For such a process, $c_{n,\mu}$ receives contributions from states with zero strangeness (such as $\pi\pi$ states) whereas $\bar{c}_{\bar{n},\mu}$ contains intermediate states with strangeness equal to -1 (such as $K\pi$ states).

Depending on the detailed choices of states, currents and kinematics in Eq. (11), finite-volume energies may exist for which $E_{\bar{n}}(L,\boldsymbol{P}_i+\boldsymbol{q}) < E_i + \omega$ or $E_n(L,\boldsymbol{P}_f-\boldsymbol{q}) < E_f - \omega$, where ω is the energy injected by the current $\mathcal{J}_A$. As a consequence, intermediate states can go on-shell, generating the long-distance parts of these matrix elements. As one might expect, such states are responsible for the dominant difference between finite-volume Euclidean and infinite-volume Minkowski correlation functions and are the focus of this work. With this in mind, a cut-off index $N(\omega)$ can be introduced such that for $\bar{n}, n \geq N(\omega)$, $E_{\bar{n}}(L,\boldsymbol{P}_i+\boldsymbol{q}) - \omega > E_i$ and $E_n(L,\boldsymbol{P}_f-\boldsymbol{q}) + \omega > E_f$, i.e. the finite-volume intermediate states are off-shell up to a current-injected energy of ω. Taking $N(\omega)$ larger than the minimum requirement poses no problem and, as explained in more detail below, will likely be advantageous in practical calculations. With this in hand, one can define

$$G_L^{\geq N}(\tau,\boldsymbol{q}) \equiv \sum_{n=N}^{\infty} c_n\, \Theta(\tau)\, e^{-[E_n(L,\boldsymbol{P}_f-\boldsymbol{q})-E_f]|\tau|} + \sum_{\bar{n}=N}^{\infty} \bar{c}_{\bar{n}}\, \Theta(-\tau)\, e^{-[E_{\bar{n}}(L,\boldsymbol{P}_i+\boldsymbol{q})-E_i]|\tau|}, \tag{12}$$

as well as

$$T_L^{\geq N}(\omega,\boldsymbol{q}) \equiv \int_{-\infty}^{\infty} d\tau\, e^{-\omega\tau}\, G_L^{\geq N}(\tau,\boldsymbol{q})\,, \tag{13}$$

$$= \sum_{n=N}^{\infty} \frac{c_n}{E_n(L,\boldsymbol{P}_f-\boldsymbol{q}) - (E_f-\omega)} + \sum_{\bar{n}=N}^{\infty} \frac{\bar{c}_{\bar{n}}}{E_{\bar{n}}(L,\boldsymbol{P}_i+\boldsymbol{q}) - (E_i+\omega)}. \tag{14}$$

The introduction of the cut-off index $N(\omega)$ has rendered the integral of the subtracted correlator $G_L^{\geq N}$, multiplied by a growing exponential $e^{-\omega\tau}$, convergent. The resulting quantity, $T_L^{\geq N}$, carries no memory of the Euclidean signature of spacetime and thus brings one closer to the stated goal of recovering $\mathcal{T}$. However, the approach is yet clearly incomplete as the intermediate states labeled from 0 to $N-1$ are not accounted for. Additionally, the finite-L effects are yet to be addressed.

The first issue can be naïvely addressed in a straightforward manner by adding back in the missing terms. Defining

$$T_L^{<N}(\omega,\boldsymbol{q}) \equiv \sum_{n=0}^{N-1} \frac{c_n}{E_n(L,\boldsymbol{P}_f-\boldsymbol{q}) - (E_f-\omega)} + \sum_{\bar{n}=0}^{N-1} \frac{\bar{c}_{\bar{n}}}{E_{\bar{n}}(L,\boldsymbol{P}_i+\boldsymbol{q}) - (E_i+\omega)}\,, \tag{15}$$

one obtains for the sum

$$T_L(\omega,\boldsymbol{q}) \equiv T_L^{<N}(\omega,\boldsymbol{q}) + T_L^{\geq N}(\omega,\boldsymbol{q})\,, \tag{16}$$

$$= \sum_{n=0}^{\infty} \frac{c_n}{E_n(L,\boldsymbol{P}_f-\boldsymbol{q}) - (E_f-\omega)} + \sum_{\bar{n}=0}^{\infty} \frac{\bar{c}_{\bar{n}}}{E_{\bar{n}}(L,\boldsymbol{P}_i+\boldsymbol{q}) - (E_i+\omega)}. \tag{17}$$

Note that the c_n and $\bar{c}_{\bar{n},AB}$ coefficients for the intermediate states 0 to $N-1$ can be separately evaluated in a lattice QCD calculation from the corresponding three-point functions, see Eqs. (9) and (10).

We need to emphasize two subtle points here. First, although $T_L^{\geq N}(\omega, \boldsymbol{q})$ is written in terms of a spectral decomposition, this is not a useful identity in practice. What is most useful is the definition of $T_L^{\geq N}(\omega, \boldsymbol{q})$ in terms of the four-point functions $G_L(\tau, \boldsymbol{q})$ calculated with lattice QCD, and the spectral decomposition of the N lowest known contributions,

$$T_L^{\geq N}(\omega, \boldsymbol{q}) \equiv \int_{-\infty}^{\infty} d\tau \, e^{-\omega\tau} \, G_L^{\geq N}(\tau, \boldsymbol{q}) \tag{18}$$

$$\equiv \int_{-\infty}^{\infty} d\tau \, e^{-\omega\tau} \, \left[G_L(\tau, \boldsymbol{q}) - G_L^{<N}(\tau, \boldsymbol{q})\right] . \tag{19}$$

This definition is what is meant in the right-hand side of Eq. (2).

The second subtle point is with regards the lowest-lying states. If a given state is stable, the one can safely add it back to the correlation function using the spectral decomposition after integration as in Eq. (15). If the state considered is above a two-particle threshold and we are considering kinematics where it may go on-shell, this contribution must be replaced by spectra and matrix elements emergent from the generalized Lüscher and Lellouch-Lüscher formalisms. We explain this point is detail in the remaining part of this section.

Both the generalized Lüscher and Lellouch-Lüscher formalisms are well known and understood, but we provide here the key equations for completeness. First, the Lüscher formalism provides a relationship between the finite-volume spectrum of two particle and the infinite-volume amplitude, and in general can be written as [51]

$$\det\left[\left(F^{[\mathcal{J}|P_i\rangle]}(P_i+q, L)\right)^{-1} + \mathcal{M}^{[\mathcal{J}|P_i\rangle]}(P_i+q)\right] = 0, \tag{20}$$

with a similar quantization condition for two-hadron states with quantum numbers of $\mathcal{O}\,|P_i\rangle$ upon $\mathcal{J} \leftrightarrow \mathcal{O}, P_i + q \to P_f - q$. Here, $\mathcal{M}^{[\mathcal{O}|P_i\rangle]}$ ($\mathcal{M}^{[\mathcal{J}|P_i\rangle]}$) is the $2 \to 2$ scattering amplitude for two-particle states with the quantum numbers of $\mathcal{O}|P_i\rangle$ ($\mathcal{J}|P_i\rangle$), and F is a known kinematic function, which we write explicitly in Sec. III.

From these two new building blocks, we can construct a matrix, $\mathcal{F}_L$, which plays an important role through out this work,

$$\mathcal{F}_L^{[\mathcal{O}|P_i\rangle]}(P_f - q) \equiv \frac{1}{F^{-1}(P_f - q, L) + \mathcal{M}^{[\mathcal{O}|P_i\rangle]}(P_f - q)}, \tag{21}$$

with a similar definition for $\mathcal{F}_L^{[\mathcal{J}|P_i\rangle]}$. It is evident, this has poles whenever Eq. (20) is satisfied, and its residues are the Lellouch-Lüscher matrices [67, 69]

$$\mathcal{R}^{[\mathcal{J}|P_i\rangle]}(\boldsymbol{P}_i + \boldsymbol{q}, p_n^*) \;=\; \lim_{E_i+\omega\to E_n} \left[(E_i + \omega - E_n)\; \mathcal{F}_L^{[\mathcal{J}|P_i\rangle]}(P_i + q)\right] . \tag{22}$$

With these, one can obtain the last ingredient needed to determine $T_L^{\leq N}$, namely the finite-volume matrix elements [67, 69]

$$|\langle P_i + q|\mathcal{J}(0)|P_i\rangle_L| = \frac{1}{\sqrt{2E_i\,L^6}}\sqrt{\mathcal{H}_{1\to 2}^{[\mathcal{J}]}(P_i+q)\mathcal{R}^{[\mathcal{J}|P_i\rangle]}(P_i+q)\mathcal{H}_{2\to 1}^{[\mathcal{J}]}(P_i+q)}. \tag{23}$$

This is the Lellouch-Lüscher formula. Here, the infinite-volume $\mathbf{1} + \mathcal{J} \to \mathbf{2}$ transition amplitudes are introduced as

$$\mathcal{H}_{1\to 2}^{[\mathcal{J}]}(P_i + q) \equiv \langle P_i + q, \mathrm{out}|\mathcal{J}_A(0)|P_i\rangle, \tag{24}$$

$$\mathcal{H}_{2\to 1}^{[\mathcal{J}]}(P_f - q) \equiv \langle P_f|\mathcal{J}_A(0)|P_f - q, \mathrm{in}\rangle. \tag{25}$$

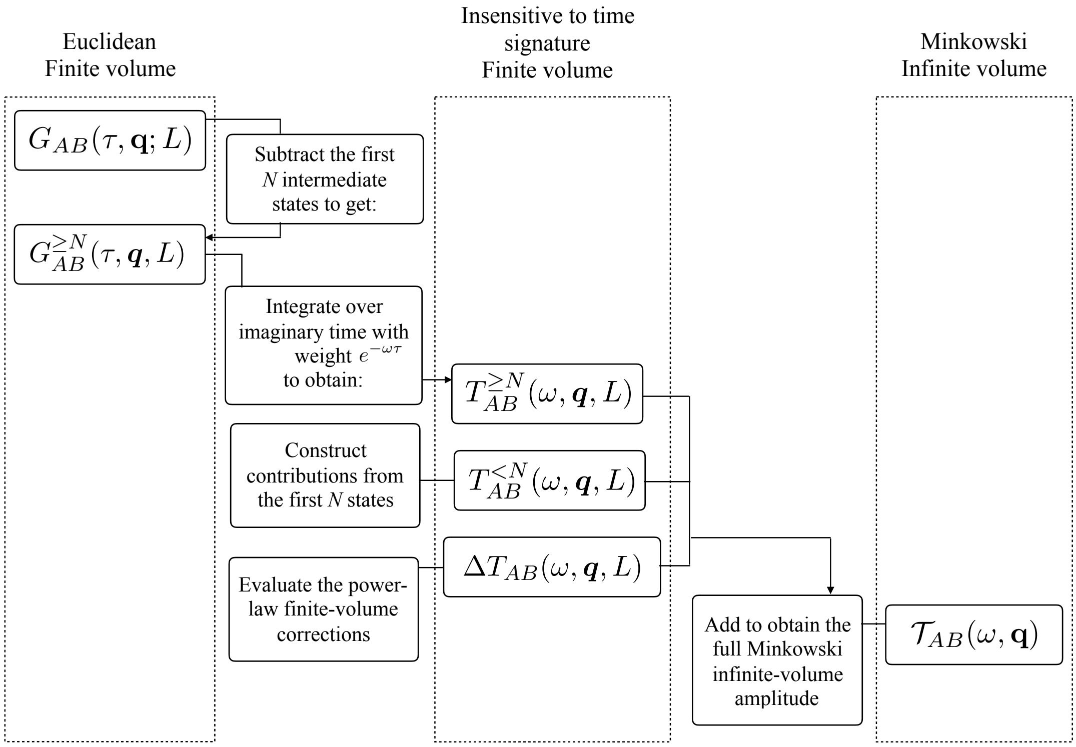

FIG. 2: $G(\tau, \boldsymbol{q}, L)$ defined in Eq. (7) is the starting point of matching the long-range bi-local matrix elements from lattice QCD to the infinite-volume Minkowski amplitude $\mathcal{T}(\omega, q)$. The intermediate quantities that must be obtained to fulfill this mapping, and the relation among them, are depicted in the chart. The P_i and P_f dependence of all functions is left implicit.

The amplitudes defined with an out-state are understood as column vectors and those with an in-state as row vectors, acting on the space of angular momentum, spin and flavor-channel space of two hadrons.

Finally, the last building block of the main equation, Eq. (2), addresses finite-volume corrections. For the kinematics considered here in which two-particle intermediate states can go on shell, the finite-volume correction is given by

$$\begin{aligned} i\Delta T(\omega, \boldsymbol{q}, L) \;\equiv\; & -i\,\mathcal{H}^{[\mathcal{J}]}_{2\to 1}(P_f - q)\,\cdot\, i\,\mathcal{F}^{[\mathcal{O}|P_i\rangle]}_{L}(P_f - q)\,\cdot\, i\,\mathcal{H}^{[\mathcal{O}]}_{1\to 2}(P_f - q) \\ & - i\,\mathcal{H}^{[\mathcal{O}]}_{2\to 1}(P_i + q)\,\cdot\, i\,\mathcal{F}^{[\mathcal{J}|P_i\rangle]}_{L}(P_i + q)\,\cdot\, i\,\mathcal{H}^{[\mathcal{J}]}_{1\to 2}(P_i + q)\,. \end{aligned} \tag{26}$$

It is worth re-emphasizing that the expressions in right-hand-side of Eq. (26) have the structure of [row vector]×[matrix]×[column vector] defined in the space of all possible degrees of freedom, including partial waves and open channels.

Given the $\mathcal{M}$, one can determine the lowest-lying energy levels. Given this and the appropriate $\mathcal{H}$'s one can proceed to evaluate the matrix elements and subsequently c_n and $\bar{c}_{\bar{n}}$ in Eq. (15). This is necessary for the pole in $T^{<N}$ and ΔT to exactly cancel and not introduce artifacts when being combined with the final term in Eq. (15). This careful interplay between these two pieces is emphasized in Eq. (2) by the "$\mathcal{M}, \mathcal{H}$" subscript. This cancelation will be illustrated in Sec. IV for a particular example.

In other words, in order to make use of Eq. (26), we need the sam exact building blocks for Eq. (15): the $1 \to 2$ transition amplitudes in Eqs. (25) and (24) and the $2 \to 2$ scattering amplitudes for the relevant initial and final states. These quantities must first be determined from dedicated lattice QCD studies using their respective finite-volume formalisms. The quantities that must be evaluated along the way of obtaining the infinite-volume Minkowski amplitude, as well the relationship among them, are depicted in Fig. 2.

III. FINITE-VOLUME CORRECTIONS TO THE FOUR-POINT CORRELATION FUNCTION

Our task now is to derive the expression for additive finite-volume correction, $\Delta T_L(\omega, \boldsymbol{q})$, given in Eq. (26). This is relatively straightforward by considering the diagrammatic representation of finite-volume correlation functions as first laid out by Kim, Sachrajda, and Sharpe (KSS) [45] in the context of identical, scalar bosons. This was indeed the starting point for Ref. [18] to study long-range effects for the study of $K - \overline{K}$ mixing. Two of the authors of the present work have since generalized the work by KSS to accommodate any number of open two-particle channels with arbitrary masses and spin [69]. Here we adopt this formalism to extend the work of Ref. [18].

To do this, we first define the desired quantity, namely the infinite-volume Minkowski amplitude, in terms of a four-momentum correlation functions using the LSZ reduction formula. The most convenient correlation functions to consider is one where we project the operators associated with the external particles and one of the external currents ($i\mathcal{J}_A$) to a definite four-momentum, while leaving the other current ($\mathcal{O}_B$) fixed at the origin,

$$\mathcal{C}(P_i, P_f, q) \equiv \int d^4x d^4y d^4z \, e^{iP_i\cdot y + iq\cdot x - iP_f\cdot z} \langle 0| \, \mathrm{T}\{\widetilde{\Psi}(z) i\mathcal{J}_A(x) i\mathcal{O}_B(0)\Psi(y)\} \, |0\rangle. \tag{27}$$

Note, the momentum of this current is fixed by momentum conservation, and this choice avoids introducing superfluous delta-functions.

The LSZ reduction assures this correlation function has poles associated with the external desired single-particle states. By amputating and placing these on-shell, we arrive at an equivalently definition of $i\mathcal{T}$, first defined in Eq. (5),

$$i\mathcal{T}(P_i, P_f, q) \equiv \lim_{P_i^0 \to E_i(\boldsymbol{P}_i), P_f^0 \to E_f(\boldsymbol{P}_f)} \left(\frac{P_i^2 - M_i^2 + i\epsilon}{i\sqrt{\mathcal{Z}_\Psi}}\right)\left(\frac{P_f^2 - M_f^2 + i\epsilon}{i\sqrt{\mathcal{Z}_{\widetilde{\Psi}}}}\right) \mathcal{C}(P_i, P_f, q), \tag{28}$$

where $\mathcal{Z}_\Psi = \langle P_i|\Psi(0)|\Omega\rangle^2$, $\mathcal{Z}_{\widetilde{\Psi}} = \langle \Omega|\widetilde{\Psi}(0)|P_f\rangle^2$. In the case of a forward amplitude, the limit $P_f \to P_i$ must be considered only after having amputated the correlation function so to remove the disconnected contributions.

Having introduced this, one can readily define a finite-volume counterpart of this correlation function,

$$C_L(P_i, P_f, q) \equiv \int_L d^4x d^4y d^4z \, e^{iP_i\cdot y + iq\cdot x - iP_f\cdot z} \langle 0| \, \mathrm{T}\{\widetilde{\Psi}(z) i\mathcal{J}_A(x) i\mathcal{O}_B(0)\Psi(y)\} \, |0\rangle_L, \tag{29}$$

where a Minkowski signature is still assumed for spacetime. Integrations over time coordinates follow as before but those over space coordinates are performed in a spatial cubic volume with periodic boundary conditions imposed on the fields. A similar LSZ reduction can be implemented with

$$iT_L(P_i, P_f, q) \equiv \lim_{P_i^0 \to E_i(\boldsymbol{P}_i), P_f^0 \to E_f(\boldsymbol{P}_f)} \left(\frac{P_i^2 - M_i^2 + i\epsilon}{i\sqrt{\mathcal{Z}_\Psi}}\right)\left(\frac{P_f^2 - M_f^2 + i\epsilon}{i\sqrt{\mathcal{Z}_{\widetilde{\Psi}}}}\right) C_L(P_i, P_f, q) \tag{30}$$

$$= \sqrt{2E_i L^3}\sqrt{2E_f L^3} \int_L d^4x \, e^{-i\omega t + i\boldsymbol{q}\cdot\boldsymbol{x}} \, \langle P_f| \, \mathrm{T}\{i\mathcal{J}_A(x) i\mathcal{O}_B(0)\} \, |P_i\rangle_{L,\mathrm{conn.}} \tag{31}$$

to arrive at the finite-volume counterpart of the Compton amplitude , namely $iT_L(P_i, P_f, q)$ ($= iT_L(\omega, \boldsymbol{q})$) [notation?] defined in the previous section.

At this point, our goal amounts to writing an exact relation between T_L and $\mathcal{T}$ up to aforementioned exponentially suppressed effects. This is exactly the quantity considered by KSS [45] and more generally again in Ref. [69]. We point the reader to this reference for a detailed description of the derivation. Here we piggyback off this work and detail the main differences.

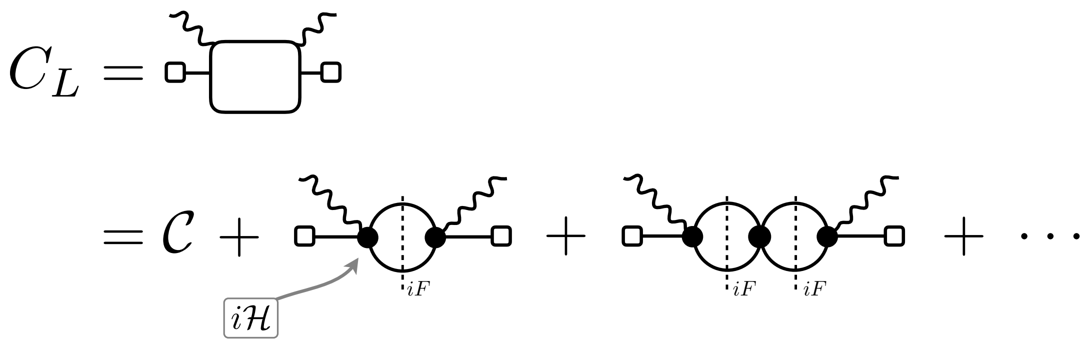

FIG. 3: Shown the the full four-point correlation function in a finite volume. In the second line we only explicitly show the s-channel diagrams, the u-channel ones follow by switching the current vertices. The notation is similar to that used in Fig. 1. The dashed lines denote contribution from the finite-volume F function, defined in Eq (34).

Equation (84) in Ref. [69] is the equation needed. There, we considered a two-point function constructed using local operators with the quantum numbers of two-particle states. Using the diagrammatic representation of the correlators we isolated all diagrams that may have power-law finite-volume effects and treat these exactly. We summed these to all orders using the same techniques developed by KSS. We then proceeded to use carefully chosen interpolating operators, see Eqs. (103) and (104) of the aforementioned reference, to relate this to three-point functions. Here we could use this same trick to obtained the desired four-point function. Instead we choose to skip ahead and simply write down the four-point from the diagrammatic representation, illustrated in Fig. 3 explicitly for s-channel diagrams. The key insight that for the kinematics considered the power-law effects appearing here as the same as those considered in arriving at Eq. (84) in Ref. [69].

One final technical point is that in Ref. [69] we chose to use Euclidean coordinates. This was perfectly reasonable, since there we were interested in the Fourier transform of the correlator. Given that here we are solely interested in Minkowski correlator this is no longer suitable. This difference is straightforward to keep track of, as we have defined all infinite- and finite-volume functions to have explicit factors of i. These factors are highlighted in Fig. 3.

Using these techniques, we sum the finite-volume corrections to all orders to arrive at

$$C_L(P_i, P_f, q) = \mathcal{C}(P_i, P_f, q) - \left(\frac{i\sqrt{\mathcal{Z}_\Psi}}{P_i^2 - M_i^2 + i\epsilon}\right) i\,\Delta T_L(P_i, P_f, q) \left(\frac{i\sqrt{\mathcal{Z}_{\widetilde{\Psi}_f}}}{P_f^2 - M_f^2 + i\epsilon}\right) \tag{32}$$

where,

$$\begin{aligned} i\Delta T_L(P_i, P_f, q) \;&=\; -i\,\mathcal{H}^{[\mathcal{J}]}_{1\to 2}(P_i+q)\,i\,\mathcal{F}_L^{[\mathcal{J}|P_i\rangle]}(P_i+q)\,i\,\mathcal{H}^{[\mathcal{O}]}_{2\to 1}(P_i+q) + \\ &\qquad \Big[\mathcal{J} \leftrightarrow \mathcal{O}, P_i + q \to P_f - q\Big], \end{aligned} \tag{33}$$

is the desired finite-volume correction to the four-point function in the kinematic region considered.

The matrix $\mathcal{F}_L^{[\mathcal{J}|P_i\rangle]}$ was defined in Eq. (21), is the geometric series depicted in Fig. 3 of produce of the scattering amplitude $\mathcal{M}$ and the finite-volume functions F, starting with the single insertion of F. These two are matrices over angular momentum and all order degrees of freedom, including open channels. In order to provide an explicit form of the finite-volume function we use the compact notation introduced in Ref. [69]. Let Jm_J be the total angular momentum and its azimuthal components, similarly S and ℓ are the spin and orbital angular

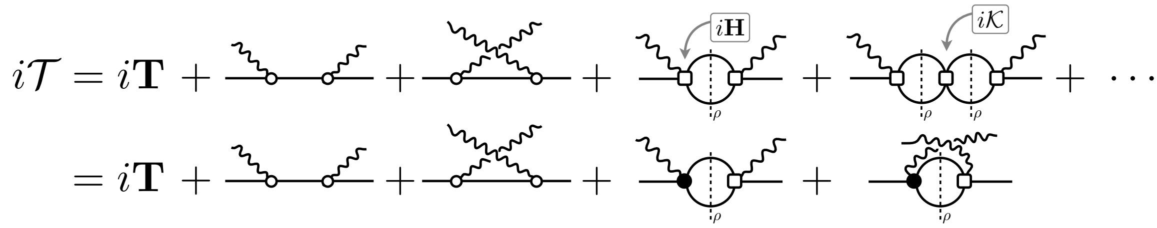

FIG. 4: Shown is the all order representation of the Compton-like amplitude, where we have isolated the contributions from imaginary parts, which are proportional to the phase space, ρ. The square vertices define the all-order transition amplitude, $\mathbf{H}$, where the principal-valued prescription has been used in the loops. These are defined in the text.

momentum. We label the channel-space using indices a and a'. With this, the F function can in general be written as [51, 69]

$$F_{\{J\},\{J'\}}(P,L) \equiv \xi_a \delta_{aa'}\delta_{SS'} \sum_{m_\ell, m'_\ell, m_S} \langle \ell\, m_\ell, S\, m_S | J m_J\rangle \langle \ell'\, m'_\ell, S'\, m_S | J' m'_J\rangle$$
$$\times \left[\frac{1}{L^3}\sum_{\mathbf{k}} - \int \frac{d\mathbf{k}}{(2\pi)^3}\right] \frac{4\pi\, Y_{\ell m_\ell}(\hat{\mathbf{k}}^*_a)\, Y^*_{\ell' m'_\ell}(\hat{\mathbf{k}}^*_a)}{2\omega_{a1} 2\omega_{a2}(E - \omega_{a1} - \omega_{a2} + i\epsilon)} \left(\frac{k^*_a}{q^*_a}\right)^{\ell+\ell'}, \quad (34)$$

where ξ_a is the symmetry factor, equal to 1/2 if the particles in channel a are identical and 1 otherwise. Labeling the particles in channel a with the numbers 1 and 2, their corresponding masses as m_{a1} and m_{a2}. Their on-shell relative-momentum in the center of mass frame is labeled q^*_a, $\omega_{a1} = \sqrt{k^2 + m^2_{a1}}$, and $\omega_{a2} = \sqrt{(\mathbf{P}-\mathbf{k})^2 + m^2_{a2}}$. [6]

Equation (33) provides the final missing piece of the main result of this work, Eq. (2). The other necessary pieces, namely the generalized Lüscher and generalized Lellouch-Lüscher formalisms have been previously derived in the literature. For completeness, here we provide a derivation of these from Eq. (33). First, the pole singularities of the finite-volume correlation function gives rise to (generalized) Lüscher's quantization condition, given in Eq. (20).

To obtain the generalized Lellouch-Lüscher relation we consider a special case of Eq. (31), where $\mathcal{J} = \mathcal{O}$ and $P_i = P_f$. Next, we evaluate T_L two different ways. First, one that more closely resembles the spectral decomposition. This amounts to evaluating the four-dimensional integral in Eq. (31). To this, we separate the integral into the two-time ordered regions, and insert a complete set of finite-volume states between these two. Since the currents and in/out states are the same, we get two identical contributions. By fixing the kinematics such that the total energy coincides with that of one of the inserted finite-volume states we arrive at,

$$\lim_{E_i+\omega\to E_n} \frac{1}{2}\, iT_L(P_i,q) = 2E_i\, L^6\, \frac{i\,|\langle \boldsymbol{P}_i + \boldsymbol{q}, E_n | i\mathcal{J}(0)|P_i\rangle_L|^2}{(E_i+\omega) - E_n}. \quad (35)$$

For the second identify of T_L, we make use of the fact that its poles come from Eq. (33),

$$\lim_{E_i+\omega\to E_n} \frac{1}{2}\, iT_L(P_i,q) = \lim_{E_i+\omega\to E_n} \left[i\,\mathcal{H}^{[\mathcal{J}]}_{1\to 2}(P_i+q)\, i\,\mathcal{F}^{[\mathcal{J}|P_i\rangle]}_L(P_i+q)\, i\,\mathcal{H}^{[\mathcal{J}]}_{2\to 1}(P_i+q)\right]. \quad (36)$$

By equation these two expressions, we arrive at Eq. (23).

[6] Note, when the "$*$" acts on a kinematic variable it denote its center of mass value, but when it acts on function it will be used to define its complex conjugate.

A. Unitarity check

As a way to provide further confidence in the quoted expression for $i\mathcal{T}$ in terms of Lattice-obtained quantities, Eq. (2), we prove here that this expression is consistent with unitarity. As argued in a more challenging case, in the context of three-particle scattering [83], in implementing all-orders-perturbation one accounts for all cuts and singularities in the kinematic region considered. These are the only sources of imaginary contributions to scattering amplitudes. As a result, if done correctly, this procedure, which is the one followed here, must be consistent with unitarity. Nevertheless, it is worthwhile checking that the emergent amplitudes are indeed in the very least consistent with unitarity.

To do this, we first write an all-order-expression for the scattering amplitude in the infinite-volume, as depicted in Fig. 4. Focusing our attention to the kinematic region where only two-particle states may go on-shell, we can analyze these diagrams by isolating systematically isolating imaginary contributions. These are only present in the two-particle s-channel loops and are proportional to the phase-space factor ρ

$$\rho_a = \frac{q_a^* \, \xi_a}{8\pi E^*}. \tag{37}$$

This arrises from $i\epsilon$ contribution of the propagators. The remaining pieces are purely real and can be associate with the same principal-valued prescribed diagrams. For the two-particle scattering amplitude, its principal-valued analogue is the K matrix, $\mathcal{K}$, and are related via

$$i\mathcal{M} = i\mathcal{K}\frac{1}{1-i\rho\mathcal{K}}, \tag{38}$$

$$= i\mathcal{K} + i\mathcal{K}\frac{1}{1-i\rho\mathcal{K}}\rho\, i\mathcal{K}, \tag{39}$$

which emergences naturally from the all-orders definition.

Similarly, we define the principal-valued prescribed $\mathcal{H}$ as $\mathbf{H}$, and these are related via

$$i\mathcal{H} = i\mathbf{H}\frac{1}{1-i\rho\mathcal{K}} \tag{40}$$

$$= i\mathbf{H} + i\mathbf{H}\frac{1}{1-i\rho\mathcal{K}}\rho\, i\mathcal{K}. \tag{41}$$

This also follows from the all-order definition. Note that the right hand sides of Eqs. (38) and (38) are the same and these are the sources of phases in the amplitudes. This is simple generalization of the Watson's theorem for any number of channels [67].

Similarly, we can go ahead and write down an expression of the Compton amplitude, which is consistent with unitarity to all orders. Here the simplest contribution is due to the intermediate single particle, which we denote to have a mass equal to m, and label its matrix element to be f suppressing any possible Lorentz structure and kinematic dependence. Defining $\mathbf{T}$ to be the principal-valued analogue of $\mathcal{T}$, we can easily write down the all-order result, which follows from Fig. 4,

$$i\mathcal{T} = if\frac{i}{s-m^2+i\epsilon}if + i\mathbf{H}\frac{1}{1-i\rho\mathcal{K}}\rho\, i\mathbf{H} + i\mathbf{T} + \text{“u-channel”}, \tag{42}$$

where s, u are the standard Mandelstam variables, “u-channel” reminds the reader that if we were to explicitly label the momenta these contributions must be taken into account. At this point, a couple of things are evidently similar between $i\mathcal{T}$ and the previously considered amplitudes. First, besides the single-particle pole, $\rho_a \sim \sqrt{s-(m_{a1}+m_{a2})^2}$ is the only other singularity in s. This *threshold* singularity is shared by all the amplitudes. Second, if there is a single channel open, the phase of the second term in $\mathcal{T}$ would be that of $\mathcal{M}$ and $\mathcal{H}$.

Below the two-particle thresholds, the phase space, Eq. (37), is purely imaginary. As a result, $\mathcal{M}$ and $\mathcal{H}$ are purely real. Similarly, the only possible imaginary contribution to the Compton amplitude is due to the single particle pole. Above two-particle thresholds, ρ is real, and consequently $\mathcal{M}$, $\mathcal{H}$, and $\mathcal{T}$ are all complex. Unitarity implies that

$$\mathrm{Im}\,[\mathcal{M}] = \mathcal{M}^*\,\overline{\rho}\,\mathcal{M}, \tag{43}$$

where $\overline{\rho}_a = \rho_a\,\Theta(s-(m_{a1}+m_{a2})^2)$. It is straightforward to check that Eq. (38) indeed satisfies this. In general, this relation reads that the imaginary contribution of an amplitude is due to intermediate particles going on-shell. It is proportional to the phase of these intermediate particles, the coupling of these to the initial state and the complex-conjugate of the coupling to the final states. For the single-current transition amplitude this reads

$$\mathrm{Im}\,[\mathcal{H}] = \mathcal{H}^*\,\overline{\rho}\,\mathcal{M}, \tag{44}$$

which is clearly consistent with Eq. (40).

Similarly, above the two-particle threshold, for the Compton amplitude this reads

$$\mathrm{Im}\,[\mathcal{T}] = +\mathcal{H}^*\,\overline{\rho}\,\mathcal{H} + \text{“u-channel”}, \tag{45}$$

which is consistent with Eq. 42 as expected.

Having done this check, we can proceed to check that this is also $\mathrm{Im}\,[\,\Delta T_L]$. This is a necessary condition for Eq. (2) to be true, since $G^{\geq N}$ and $T^{<N}$ are purely real. Starting from Eq. (26),

$$\begin{aligned}
\mathrm{Im}\,[\,\Delta T_L] &= \mathrm{Im}\,[\mathcal{H}\ \mathcal{F}_L\,\mathcal{H}] + \text{“u-channel”} &(46)\\
&= \left(\mathcal{H}^*\mathcal{M}^{*-1}\right)\mathrm{Im}\left[\mathcal{M}\,F\ \frac{1}{\mathcal{M}^{-1}+F}\right]\left(\mathcal{M}^{-1}\mathcal{H}\right) + \text{“u-channel”} &(47)\\
&= \left(\mathcal{H}^*\mathcal{M}^{*-1}\right)\mathrm{Im}\,[\mathcal{M}\,F\,]\ \frac{1}{\mathcal{K}^{-1}+F_{\mathrm{PV}}}\left(\mathcal{M}^{-1}\mathcal{H}\right) + \text{“u-channel”} &(48)\\
&= \left(\mathcal{H}^*\mathcal{M}^{*-1}\right)[\mathcal{M}^*\overline{\rho}\mathcal{M}\,F + \mathcal{M}^*\overline{\rho}]\ \frac{1}{\mathcal{K}^{-1}+F_{\mathrm{PV}}}\left(\mathcal{M}^{-1}\mathcal{H}\right) + \text{“u-channel”} &(49)\\
&= \mathcal{H}^*\,\overline{\rho}\,\mathcal{H} + \text{“u-channel”}, &(50)
\end{aligned}$$

where we used the fact that $\mathrm{Im}\,[F] = -\mathrm{Im}\left[\mathcal{M}^{-1}\right] = \overline{\rho}$, which evident from the definition Eq.(34). For clarity, in parenthesis we wrote products of amplitudes are purely real.

In summary, we have shown that the imaginary piece of the right hand of Eq. (2) is consistent with the expectation from unitarity. Furthermore, we have provided a functional form of the Compton amplitude that emerges from all-order in perturbation theory and is consequently also consistent with unitarity. As emphasized in the previous section, to make use of this formalism one must first determine all observables associated with the subprocesses. This means that in Eq. (42) all building blocks are in-principle known except for $\mathbf{T}$, which can be understood as the target observable of a dedicated study of four-point functions. In Sec. IV we discuss in further detail and mention one subtlety when considered amplitudes where the K matrix has real-values poles.

IV. NUMERICAL IMPLEMENTATION

Having derived all necessary elements for a systematic four-point function study above any number of two-particle thresholds, here we consider an illustrative numerical example of the the simplest nontrivial case. In particular, we consider kinematics where only one channel is open, composed of two identical scalar particles with mass m. This means that $\xi = 1/2$. Furthermore, we perform a partial-wave decomposition and assume that only the lowest partial wave ($\ell = 0$)

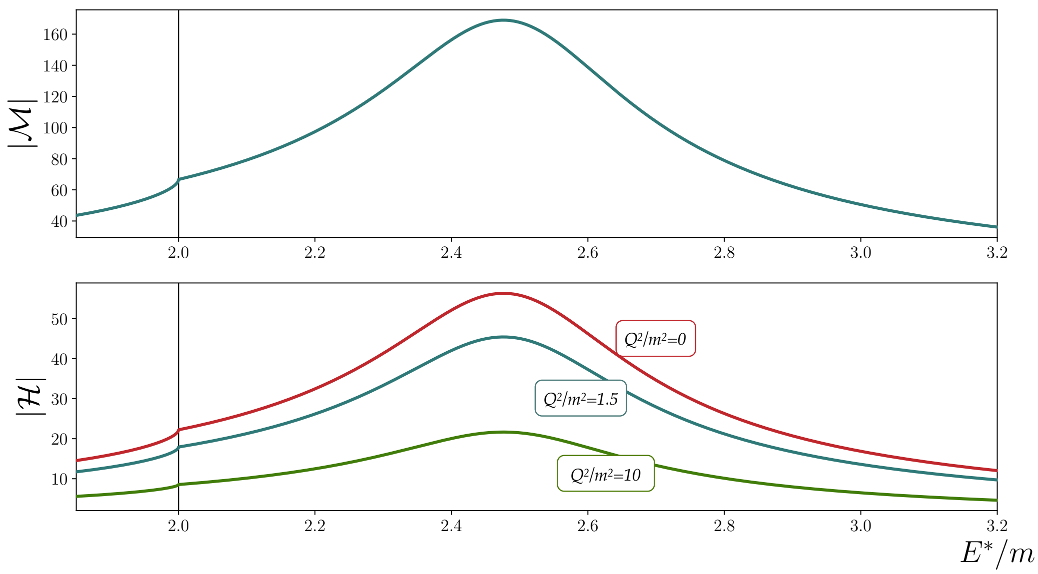

FIG. 5: Magnitude squared of the scattering amplitude (upper panel) and $1+\mathcal{J}\to 2$ transition amplitude (lower panel) using $m_R = 2.5\,m$ and $g = 3.0$ in the functions defined in the text. Three representative values of momentum transfer are shown for the transition amplitude.

contributes. The current considered is scalar, as a result the single-particle state has a single form factor and $1 \to 2$ transition amplitude has a single Lorentz scalar amplitude.

Here we make use of the expressions where unitarity is already incorporated in the definition of the amplitudes. This implies that for $\mathcal{M}$ we just need to parametrize the K matrix. We first write this in terms of the scattering phase shift,

$$\mathcal{K}(P^2) = \frac{16\pi E^*}{q^*}\frac{1}{\cot\delta(q^*)}. \tag{51}$$

$$\tag{52}$$

We proceed to parametrize the phase shift in terms of the S-wave Breit-Wigner function,

$$\tan\delta(q^*) = \frac{E^*\,\Gamma(E^*)}{m_R^2 - E^{*2}}, \tag{53}$$

$$\Gamma(E^*) = \frac{g^2}{6\pi}\frac{m_R^2}{E^{*2}}q^*, \tag{54}$$

where m_R qualitatively related to the mass of the resonance and g the coupling to the two-particle states. For all following numerical results we fix $m_R = 2.5m$ and $g = 3.0$, and we can see in Fig. 5 that standard peak-like structure near $E^{*2} \sim m_R^2$ and the cusp right at threshold.

In this limit, where a single partial wave contributes, the quantization condition, Eq. (20) becomes a simple algebraic equation,

$$\mathcal{M}(P^2) = -F^{-1}(P, L). \tag{55}$$

The corresponding finite-volume spectrum is shown in Fig. 6 for two choices of the three momentum, where the light blue lines indicate the noninteracting case, while the red lines correspond to the interacting theory.

From Eq. (40), we see that given $\mathcal{K}$ we still need $\mathbf{H}$ to define the full $1 \to 2$ transition amplitude. Unitarity and all-order perturbation theory require that $\mathbf{H}(Q^2, P^2)$ has a pole if $\mathcal{K}(P^2)$ does [84]. Such a pole is not physical and is a consequence of the parametrization. This motivates rewriting

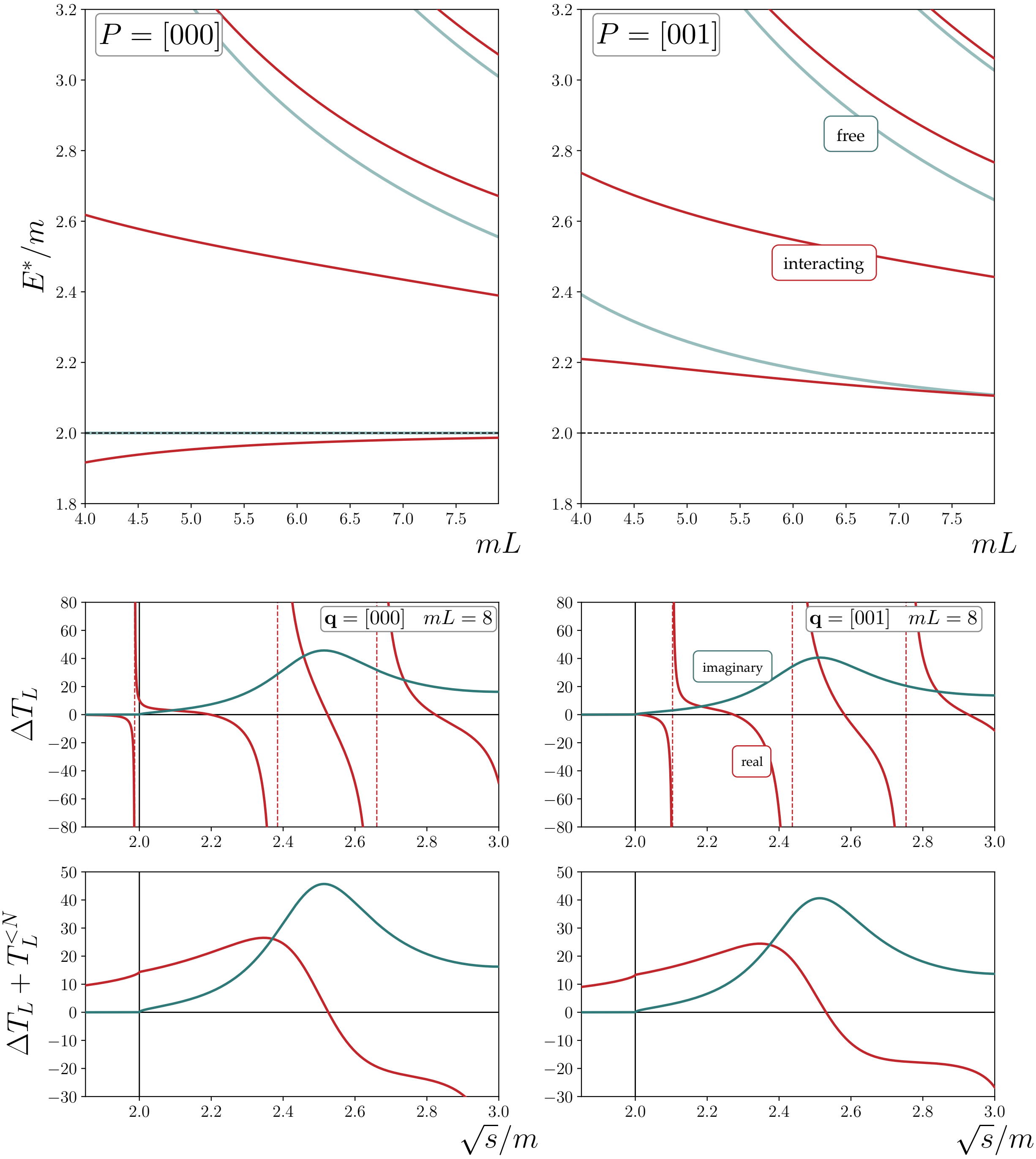

FIG. 6: Top panel: Finite-volume spectrum for two values of the spatial momentum. The blue lines show the result for the free theory, while the red lines correspond to the interacting theory with $\mathcal{M}$ given in Fig. 5. Middle panel: ΔT as defined in Eq. (26), given $\mathcal{M}$ and $\mathcal{H}$ in Fig. 5, where initial and final states are fixed to be at rest. Bottom panel: the additive term defined in Eq. (2).

$\mathbf{H}(Q^2, P^2)$ in the form [85, 86]

$$\mathbf{H}(Q^2, P^2) = \mathbf{F}(Q^2, P^2)\mathcal{K}(P^2), \tag{56}$$

where $\mathbf{F}_\ell(Q^2, P^2)$ is a smooth function. Here we fix it to be $\mathbf{F}_\ell(Q^2, P^2) = f(Q^2)/3$, where $f(Q^2)$

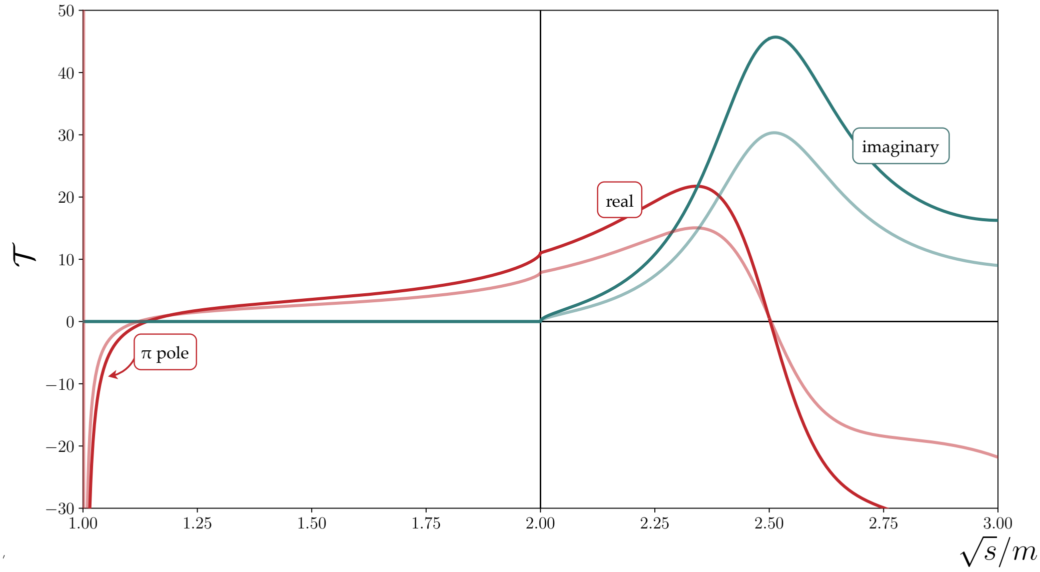

FIG. 7: Real (red line) and imaginary part (blue line) of the Compton amplitude. The initial and final states are fixed to be at rest. The darker lines correspond to currents have zero momentum, the faded lines correspond to $q = 2\pi[001]/L$ where $mL = 8$ to match the functions illustrated in Fig. 6.

is the single particle form factor, which we parametrize by a simple time-like pole,

$$f(Q^2) = \frac{m_R^2}{m_R^2 + Q^2}. \tag{57}$$

In the second panel of Fig. 5, we plot $\mathcal{H}$ for a range of kinematics.

Having both $\mathcal{M}$ and $\mathcal{H}$, we now determine ΔT, see Eq. (26). This is given in Fig. 6 for the largest volume considered in Fig. 6 and the same two boosts. Note, the real part of the function has a series of poles, these coincide with the energy levels in Fig. 6, which was used in Sec. III to derive and Eqs. (20) and (23). The imaginary piece has a cusp at threshold and the same peak structure as the $\mathcal{M}$ and $\mathcal{H}$. This is consistent with the fact that Im $[\Delta T_L]$ satisfies Eq. (50). Furthermore, given Eqs. (23) and (9), we can calculated $T^{<N}$. This, of course, is a sum of real-valued poles. In the second panel of Fig. 6, we plot the sum of this with ΔT_L. Here we observe the careful cancelation of the poles which was emphasized at the end of Sec. II.

To confirm that imaginary part of ΔT_L is equal to that of $\mathcal{T}$, we proceed to construct the latter. This follows from Eq. (42). Here we address a subtlety foreshadowed at the end of Sec. III A. This is with regards to the case where $\mathcal{K}_\ell$ has a pole. In such a case, we see that the second term in Eq. (42) appears to have a real-valued pole, taking the form

$$i\mathbf{H}\frac{1}{1 - i\rho\mathcal{K}}\rho\, i\mathbf{H} \sim -\mathbf{F}\mathcal{K}(P^2)\mathbf{F}. \tag{58}$$

However, in the full Compton amplitude this real pole is exactly canceled by a pole in $\mathbf{T}(P_f, q, P_i)$, which motivates parameterizing the principal-value analogue as

$$\mathbf{T} = \mathbf{F}\,\mathcal{K}\,\mathbf{F} + \text{“u-channel”} + \mathbf{S}, \tag{59}$$

where $\mathbf{S}$ is a smooth function in the region of interest. This means that in this kinematic region, the analytic structure of the Compton amplitude is given purely in terms of known functions, plus additional smooth contributions, $\mathbf{S}$. In what follows we set this contribution to be equal to 0.

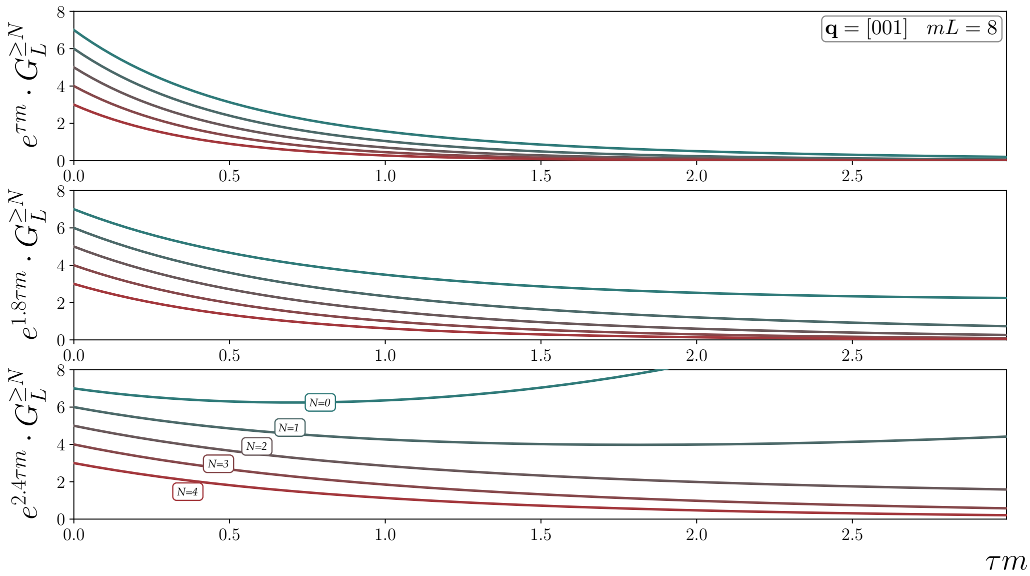

FIG. 8: Shown is the integrand of Eq. (18) for range of values of N, where initial and final states are fixed to be at rest. The color coding in the upper two panels corresponds to that of the lower panel.

Having defined the purely real contribution to the Compton amplitude, we plot the s-channel contributions in Fig. 7. We observe the expected result that its imaginary contribution agrees with that of ΔT_L, shown in Fig. 6.

As a final illustration of the proposed formalism, in Fig. 8 we plot the subtracted correlation function, i.e. $G_L^{\geq N}$ for a set of kinematics and a range of subtractions as a function of Euclidean time. This is the integrand of $T_L^{\geq N}$, defined in Eq. (18). This illustrates the expect behavior: the larger number of subtractions one performs, the more convergent is the integral. We consider two examples where the original integral was not convergent, and after a small number of subtractions it resulted convergent. Furthermore, while one of the main goals of the proposed method is to subtract pole contributions in a specific kinematical region, additional subtractions can be performed to improve upon the convergence of the integral, as shown in the first panel of Fig. 8.

V. CONCLUSION AND OUTLOOK

The formalism presented in this work offers a path from Euclidean finite-volume correlation functions of time-displaced local electroweak currents to long-range contributions to hadronic amplitudes in an infinite Minkowski spacetime. This approach generalizes and extends the formalism of Refs. [16–18]. Given the complicated nature of the desired amplitudes, it should not be too surprising that the relation derived in this paper requires a detailed understanding of various building blocks on both ends of the mapping. Figure 9 summarizes the conclusions of this work, and provides guidance on how lattice QCD quantities may be used to access the physical infinite-volume amplitudes of interest.

The main result is given in Eq. (2). In short, we have identified an extract of the original correlation function that is independent of the time signature in the theory, denoted in Fig. 9 as the subtracted one-body matrix element. This is achieved by removing contributions to the finite-volume four-point correlation function that arise from the N lowest-lying intermediate states, including all the states that can go on shell. We then provide a close form for the necessary additive piece, $\left[T^{<N} + \Delta T\right]_{\mathcal{M},\mathcal{H}}$ in Eq. (2), which not only removes all power-law finite-volume effects but restores the correct analytic structure of the infinite-volume Minkowski amplitude. This additive piece can be evaluated separately from dedicated lattice QCD studies of two- and

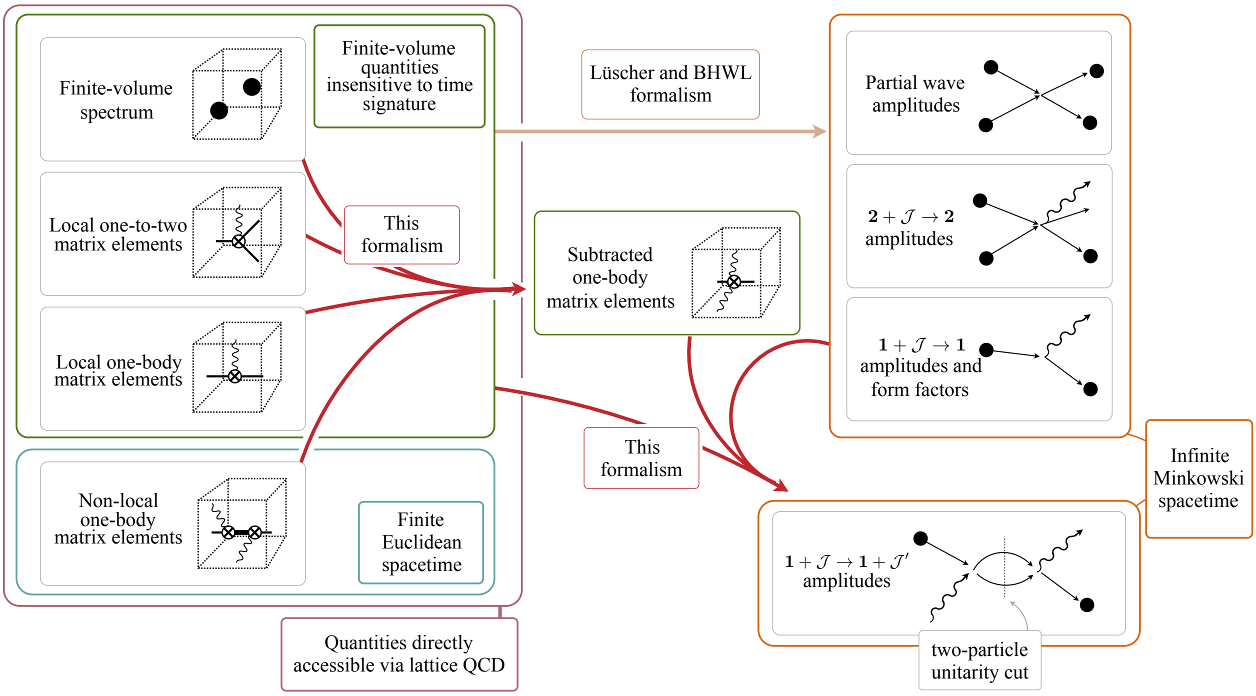

FIG. 9: Schematic map of the formalism outlined in this work. To extract the infinite-volume Minkowski amplitude involving two currents, a number of building blocks have to be determined with lattice QCD (shown on the left of the figure), including the spectrum and transition amplitudes with single currents. The red arrows show how these building blocks are combined in the current formalism.

three-point functions.

The results presented hold not only for single-hadron long-range electroweak transitions, but also for transitions involving the vacuum in the initial/final states, such as for matrix element incurred in studying the QCD structure of the photon [33]. Arbitrary quantum numbers, such as spin, flavor, partial waves and total CM momentum, are incorporated in this general formalism, and the possibility of multiple coupled partial-wave or flavor channels in intermediate two-hadron states is accounted for. An explicit map of the workflow for future numerical implementation of the formalism is shown in Fig. 2, with a reference to quantities that are defined in various equations throughout this paper.

The general form of our result can also serve as guidance on how to address further issues, such as extending the kinematic reach or considering two-hadron initial and final states, which will be relevant for neutrinoful and neutrinoless double-beta decay studies [87]. Furthermore, extension to kinematic regions beyond the three-hadron productions may be possible, and they could naturally extended from the recently-developed technologies for the determination of the spectrum [76–81, 84, 88–95]. More immediately, one can imagine extending these ideas for processes like $\gamma^*\gamma^* \to \pi\pi$, which would be relevant for dispersive analysis of the hadronic light-by-light contribution (HLbL) to muon $g-2$ [96]. These will need to build off this work as well as parallel work for the study of two-body finite-volume matrix elements [70, 71].

VI. ACKNOWLEDGEMENTS

RAB is supported in part by USDOE grant No. DE-AC05-06OR23177, under which Jefferson Science Associates, LLC, manages and operates Jefferson Lab. RAB also acknowledges support from the USDOE Early Career award, contract de-sc0019229.

---

[1] X.-D. Ji, Phys. Rev. **D55**, 7114 (1997), hep-ph/9609381.
[2] S. Dell'Oro, S. Marcocci, M. Viel, and F. Vissani, Adv. High Energy Phys. **2016**, 2162659 (2016), 1601.07512.
[3] M. J. Dolinski, A. W. P. Poon, and W. Rodejohann, Submitted to: Ann. Rev. Nucl. Part. Phys. (2019), 1902.04097.
[4] R. Henning, Rev. Phys. **1**, 29 (2016).
[5] W. Rodejohann, Int. J. Mod. Phys. **E20**, 1833 (2011), 1106.1334.
[6] G. Prezeau, M. Ramsey-Musolf, and P. Vogel, Phys. Rev. **D68**, 034016 (2003), hep-ph/0303205.
[7] J. Menendez, D. Gazit, and A. Schwenk, Phys. Rev. Lett. **107**, 062501 (2011), 1103.3622.
[8] V. Cirigliano, W. Dekens, E. Mereghetti, and A. Walker-Loud (2017), 1710.01729.
[9] V. Cirigliano, W. Dekens, J. De Vries, M. L. Graesser, E. Mereghetti, S. Pastore, and U. Van Kolck (2018), 1802.10097.
[10] V. Cirigliano, W. Dekens, J. de Vries, M. L. Graesser, and E. Mereghetti (2018), 1806.02780.
[11] A. Nicholson et al., Phys. Rev. Lett. **121**, 172501 (2018), 1805.02634.
[12] P. E. Shanahan, B. C. Tiburzi, M. L. Wagman, F. Winter, E. Chang, Z. Davoudi, W. Detmold, K. Orginos, and M. J. Savage, Phys. Rev. Lett. **119**, 062003 (2017), 1701.03456.
[13] B. C. Tiburzi, M. L. Wagman, F. Winter, E. Chang, Z. Davoudi, W. Detmold, K. Orginos, M. J. Savage, and P. E. Shanahan, Phys. Rev. **D96**, 054505 (2017), 1702.02929.
[14] X. Feng, L.-C. Jin, X.-Y. Tuo, and S.-C. Xia (2018), 1809.10511.
[15] W. Detmold and D. J. Murphy, PoS **LATTICE2018**, 262 (2019), 1811.05554.
[16] N. H. Christ (RBC Collaboration, UKQCD Collaboration) (2010), 1012.6034.
[17] N. Christ, G. Martinelli, and C. Sachrajda, PoS **LATTICE2013**, 399 (2014), 1401.1362.
[18] N. H. Christ, X. Feng, G. Martinelli, and C. T. Sachrajda, Phys. Rev. **D91**, 114510 (2015), 1504.01170.
[19] Z. Bai, N. H. Christ, and C. T. Sachrajda, EPJ Web Conf. **175**, 13017 (2018).
[20] N. H. Christ, X. Feng, A. Juttner, A. Lawson, A. Portelli, and C. T. Sachrajda, Phys. Rev. **D94**, 114516 (2016), 1608.07585.
[21] Z. Bai, N. H. Christ, X. Feng, A. Lawson, A. Portelli, and C. T. Sachrajda, Phys. Rev. Lett. **118**, 252001 (2017), 1701.02858.
[22] Z. Bai, N. H. Christ, X. Feng, A. Lawson, A. Portelli, and C. T. Sachrajda, Phys. Rev. **D98**, 074509 (2018), 1806.11520.
[23] C. Lehner et al. (2019), 1904.09479.
[24] V. Cirigliano, Z. Davoudi, T. Bhattacharya, T. Izubuchi, P. E. Shanahan, S. Syritsyn, and M. L. Wagman (2019), 1904.09704.
[25] W. Detmold, R. G. Edwards, J. J. Dudek, M. Engelhardt, H.-W. Lin, S. Meinel, K. Orginos, and P. Shanahan (2019), 1904.09512.
[26] A. S. Kronfeld, D. G. Richards, W. Detmold, R. Gupta, H.-W. Lin, K.-F. Liu, A. S. Meyer, R. Sufian, and S. Syritsin (USQCD) (2019), 1904.09931.
[27] T. Pichler, M. Dalmonte, E. Rico, P. Zoller, and S. Montangero, Physical Review X **6**, 011023 (2016).
[28] A. Alexandru, G. Basar, P. F. Bedaque, S. Vartak, and N. C. Warrington, Phys. Rev. Lett. **117**, 081602 (2016), 1605.08040.
[29] E. A. Martinez et al., Nature **534**, 516 (2016), 1605.04570.
[30] N. Klco, E. F. Dumitrescu, A. J. McCaskey, T. D. Morris, R. C. Pooser, M. Sanz, E. Solano, P. Lougovski, and M. J. Savage, Phys. Rev. **A98**, 032331 (2018), 1803.03326.
[31] R. A. Briceño, M. T. Hansen, and C. J. Monahan, Phys. Rev. **D96**, 014502 (2017), 1703.06072.
[32] R. A. Briceno, J. V. Guerrero, M. T. Hansen, and C. J. Monahan, Phys. Rev. **D98**, 014511 (2018), 1805.01034.
[33] X.-d. Ji and C.-w. Jung, Phys. Rev. Lett. **86**, 208 (2001), hep-lat/0101014.
[34] H. B. Meyer, Eur. Phys. J. **A49**, 84 (2013), 1303.0138.
[35] J. J. Dudek and R. G. Edwards, Phys. Rev. Lett. **97**, 172001 (2006), hep-ph/0607140.
[36] A. Gerardin, H. B. Meyer, and A. Nyffeler, Phys. Rev. **D94**, 074507 (2016), 1607.08174.
[37] A. Gerardin, H. B. Meyer, and A. Nyffeler (2019), 1903.09471.
[38] T. Izubuchi, Y. Kuramashi, C. Lehner, and E. Shintani (PACS), Phys. Rev. **D98**, 054505 (2018), 1805.04250.
[39] A. Gerardin, M. Cè, G. von Hippel, B. Hörz, H. B. Meyer, D. Mohler, K. Ottnad, J. Wilhelm, and

H. Wittig (2019), 1904.03120.
[40] N. Christ, T. Izubuchi, C. Sachrajda, A. Soni, and J. Yu (RBC and UKQCD Collaborations), Phys.Rev. **D88**, 014508 (2013), 1212.5931.
[41] Z. Bai, N. Christ, T. Izubuchi, C. Sachrajda, A. Soni, et al., Phys.Rev.Lett. **113**, 112003 (2014), 1406.0916.
[42] N. Christ, T. Izubuchi, C. T. Sachrajda, A. Soni, and J. Yu (RBC, UKQCD), PoS **LATTICE2013**, 397 (2014), 1402.2577.
[43] M. Luscher, Nucl.Phys. **B354**, 531 (1991).
[44] K. Rummukainen and S. A. Gottlieb, Nucl. Phys. **B450**, 397 (1995), hep-lat/9503028.
[45] C. Kim, C. Sachrajda, and S. R. Sharpe, Nucl.Phys. **B727**, 218 (2005), hep-lat/0507006.
[46] S. He, X. Feng, and C. Liu, JHEP **07**, 011 (2005), hep-lat/0504019.
[47] Z. Davoudi and M. J. Savage, Phys. Rev. **D84**, 114502 (2011), 1108.5371.
[48] M. T. Hansen and S. R. Sharpe, Phys.Rev. **D86**, 016007 (2012), 1204.0826.
[49] R. A. Briceño and Z. Davoudi, Phys. Rev. D. 88, **094507**, 094507 (2013), 1204.1110.
[50] R. A. Briceño, Z. Davoudi, and T. C. Luu, Phys. Rev. **D88**, 034502 (2013), 1305.4903.
[51] R. A. Briceño, Phys.Rev. **D89**, 074507 (2014), 1401.3312.
[52] D. J. Wilson, R. A. Briceño, J. J. Dudek, R. G. Edwards, and C. E. Thomas, Phys. Rev. **D92**, 094502 (2015), 1507.02599.
[53] R. A. Briceño, J. J. Dudek, R. G. Edwards, and D. J. Wilson, Phys. Rev. Lett. **118**, 022002 (2017), 1607.05900.
[54] R. Brett, J. Bulava, J. Fallica, A. Hanlon, B. Hörz, and C. Morningstar, Nucl. Phys. **B932**, 29 (2018), 1802.03100.
[55] D. Guo, A. Alexandru, R. Molina, M. Mai, and M. Döring, Phys. Rev. **D98**, 014507 (2018), 1803.02897.
[56] C. W. Andersen, J. Bulava, B. Hörz, and C. Morningstar, Phys. Rev. **D97**, 014506 (2018), 1710.01557.
[57] C. Andersen, J. Bulava, B. Hörz, and C. Morningstar, Nucl. Phys. **B939**, 145 (2019), 1808.05007.
[58] J. J. Dudek, R. G. Edwards, C. E. Thomas, and D. J. Wilson (2014), 1406.4158.
[59] J. J. Dudek, R. G. Edwards, and D. J. Wilson (Hadron Spectrum), Phys. Rev. **D93**, 094506 (2016), 1602.05122.
[60] A. Woss, C. E. Thomas, J. J. Dudek, R. G. Edwards, and D. J. Wilson, JHEP **07**, 043 (2018), 1802.05580.
[61] A. J. Woss, C. E. Thomas, J. J. Dudek, R. G. Edwards, and D. J. Wilson (2019), 1904.04136.
[62] K. Orginos, A. Parreno, M. J. Savage, S. R. Beane, E. Chang, and W. Detmold, Phys. Rev. **D92**, 114512 (2015), 1508.07583.
[63] E. Berkowitz, T. Kurth, A. Nicholson, B. Joo, E. Rinaldi, M. Strother, P. M. Vranas, and A. Walker-Loud, Phys. Lett. **B765**, 285 (2017), 1508.00886.
[64] M. L. Wagman, F. Winter, E. Chang, Z. Davoudi, W. Detmold, K. Orginos, M. J. Savage, and P. E. Shanahan, Phys. Rev. **D96**, 114510 (2017), 1706.06550.
[65] L. Lellouch and M. Luscher, Commun.Math.Phys. **219**, 31 (2001), hep-lat/0003023.
[66] H. B. Meyer, Phys. Rev. Lett. **107**, 072002 (2011), 1105.1892.
[67] R. A. Briceño, M. T. Hansen, and A. Walker-Loud (2014), 1406.5965.
[68] X. Feng, S. Aoki, S. Hashimoto, and T. Kaneko, Phys. Rev. **D91**, 054504 (2015), 1412.6319.
[69] R. A. Briceño and M. T. Hansen, Phys. Rev. **D92**, 074509 (2015), 1502.04314.
[70] R. A. Briceño and M. T. Hansen, Phys. Rev. **D94**, 013008 (2016), 1509.08507.
[71] A. Baroni, R. A. Briceño, M. T. Hansen, and F. G. Ortega-Gama (2018), 1812.10504.
[72] R. A. Briceño, J. J. Dudek, and R. D. Young, Rev. Mod. Phys. **90**, 025001 (2018), 1706.06223.
[73] T. Yamazaki, PoS **LATTICE2014**, 009 (2015), 1503.08671.
[74] Z. Davoudi, EPJ Web Conf. **175**, 01022 (2018), 1711.02020.
[75] Z. Davoudi, PoS **LATTICE2018**, 014 (2018), 1812.11899.
[76] M. T. Hansen and S. R. Sharpe, Phys.Rev. **D90**, 116003 (2014), 1408.5933.
[77] M. T. Hansen and S. R. Sharpe, Phys. Rev. **D92**, 114509 (2015), 1504.04248.
[78] M. Mai and M. Doring, Eur. Phys. J. **A53**, 240 (2017), 1709.08222.
[79] H. W. Hammer, J. Y. Pang, and A. Rusetsky, JHEP **10**, 115 (2017), 1707.02176.
[80] R. A. Briceño, M. T. Hansen, and S. R. Sharpe, Phys. Rev. **D95**, 074510 (2017), 1701.07465.
[81] T. D. Blanton, F. Romero-López, and S. R. Sharpe, JHEP **03**, 106 (2019), 1901.07095.
[82] F. Romero-Lopez, S. R. Sharpe, T. D. Blanton, R. A. Briceno, and M. T. Hansen (2019), 1908.02411.
[83] R. A. Briceno, M. T. Hansen, S. R. Sharpe, and A. P. Szczepaniak (2019), 1905.11188.
[84] R. A. Briceño, M. T. Hansen, and S. R. Sharpe, Phys. Rev. **D99**, 014516 (2019), 1810.01429.
[85] R. A. Briceño, J. J. Dudek, R. G. Edwards, C. J. Shultz, C. E. Thomas, and D. J. Wilson, Phys.

Rev. Lett. **115**, 242001 (2015), 1507.06622.
[86] R. A. Briceño, J. J. Dudek, R. G. Edwards, C. J. Shultz, C. E. Thomas, and D. J. Wilson, Phys. Rev. **D93**, 114508 (2016), 1604.03530.
[87] V. Cirigliano, W. Dekens, J. de Vries, M. L. Graesser, E. Mereghetti, S. Pastore, M. Piarulli, U. van Kolck, and R. B. Wiringa (2019), 1907.11254.
[88] K. Polejaeva and A. Rusetsky, Eur.Phys.J. **A48**, 67 (2012), 1203.1241.
[89] R. A. Briceño and Z. Davoudi, Phys.Rev. **D87**, 094507 (2013), 1212.3398.
[90] H.-W. Hammer, J.-Y. Pang, and A. Rusetsky, JHEP **09**, 109 (2017), 1706.07700.
[91] P. Guo and V. Gasparian, Phys. Lett. **B774**, 441 (2017), 1701.00438.
[92] M. Doring, H. W. Hammer, M. Mai, J. Y. Pang, A. Rusetsky, and J. Wu, Phys. Rev. **D97**, 114508 (2018), 1802.03362.
[93] R. A. Briceño, M. T. Hansen, and S. R. Sharpe, Phys. Rev. **D98**, 014506 (2018), 1803.04169.
[94] M. Mai and M. Doring, Phys. Rev. Lett. **122**, 062503 (2019), 1807.04746.
[95] M. T. Hansen and S. R. Sharpe (2019), 1901.00483.
[96] G. Colangelo, M. Hoferichter, M. Procura, and P. Stoffer, JHEP **09**, 074 (2015), 1506.01386.